Prophase I arrest and progression to metaphase I in mouse oocytes are controlled by Emi1-dependent regulation of APC^{Cdh1}

Petros Marangos,[1] Emmy W. Verschuren,[2] Ruby Chen,[3] Peter K. Jackson,[2] and John Carroll[1]

[1]Department of Physiology, University College London, London WC1E 6BT, England, UK
[2]Department of Pathology, School of Medicine, and [3]Department of Obstetrics and Gynecology, Division of Reproductive Biology, Stanford University, Palo Alto, CA 94305

Mammalian oocytes are arrested in prophase of the first meiotic division. Progression into the first meiotic division is driven by an increase in the activity of maturation-promoting factor (MPF). In mouse oocytes, we find that early mitotic inhibitor 1 (Emi1), an inhibitor of the anaphase-promoting complex (APC) that is responsible for cyclin B destruction and inactivation of MPF, is present at prophase I and undergoes Skp1–Cul1–F-box/βTrCP-mediated destruction immediately after germinal vesicle breakdown (GVBD). Exogenous Emi1 or the inhibition of Emi1 destruction in prophase-arrested oocytes leads to a stabilization of cyclin B1–GFP that is sufficient to trigger GVBD. In contrast, the depletion of Emi1 using morpholino oligonucleotides increases cyclin B1–GFP destruction, resulting in an attenuation of MPF activation and a delay of entry into the first meiotic division. Finally, we show that Emi1-dependent effects on meiosis I require the presence of Cdh1. These observations reveal a novel mechanism for the control of entry into the first meiotic division: an Emi1-dependent inhibition of APC^{Cdh1}.

Introduction

Meiosis in mammalian oocytes is driven by changes in the activity of maturation-promoting factor (MPF). MPF activity is attributed entirely to the activity of the universal mitotic kinase, cdk1–cyclin B (Draetta et al., 1989; Labbe et al., 1989; Gautier et al., 1990). In mammals, oocytes are arrested in prophase of meiosis I with low levels of MPF (Hashimoto and Kishimoto, 1986; Choi et al., 1991). An increase in MPF activity stimulates entry into M phase of meiosis I, the first sign of which is germinal vesicle (GV) breakdown (GVBD), which takes place ∼90 min after release from the follicle. Continued cyclin B synthesis and increasing levels of MPF drive the oocyte to metaphase of the first meiotic division (Tay et al., 2000; Ledan et al., 2001), which is followed by polar body extrusion 7–9 h after GVBD. After MI, the oocyte proceeds immediately to meiosis II, where it arrests with high levels of MPF activity that are stabilized by cytostatic factor (CSF; Masui and Markert, 1971; Hashimoto and Kishimoto, 1986; Kubiak et al., 1993; Tunquist and Maller, 2003). The MI→MII transition is characterized by a transient decrease in MPF activity brought about by the destruction of cyclin B (Hashimoto and Kishimoto, 1986; Ledan et al., 2001; Herbert et al., 2003; Marangos and Carroll, 2004a). Cyclin degradation is stimulated in meiosis and mitosis by the anaphase-promoting complex (APC), an E3 ubiquitin ligase for which several mitotic proteins, including cyclin B, are substrates. The APC-catalyzed formation of a ubiquitin chain on cyclin B marks it for destruction by the 26S proteasome, and the inactivation of MPF rapidly follows (Glotzer et al., 1991; King et al., 1996; Fang et al., 1999; Zachariae and Nasmyth, 1999).

Regulation of cdk1 by cyclin availability requires that the APC is tightly regulated so as to destroy cyclin B (and its other substrates) in a timely manner (Peters, 2002). Not surprisingly, therefore, the APC is subject to a variety of regulatory mechanisms. APC activity requires one of two positive regulators, Cdc20 and Cdh1, that are required for APC activity in mitosis and late mitosis/G1, respectively (Kramer et al., 1998; Lorca et al., 1998; Raff et al., 2002; Chang et al., 2004). It is also positively regulated by cdk1–cyclin B–dependent phosphorylation, thereby providing a feedback loop that ensures a rapid exit from metaphase (Felix et al., 1990; Golan et al., 2002). Inactivation of the APC is mediated by several proteins that make up the spindle assembly checkpoint

Correspondence to Petros Marangos: p.marangos@ucl.ac.uk; or John Carroll: j.carroll@ucl.ac.uk

Abbreviations used in this paper: APC, anaphase-promoting complex; cRNA, complementary RNA; CSF, cytostatic factor; Emi1, early mitotic inhibitor 1; GV, germinal vesicle; GVBD, GV breakdown; hCG, human chorionic gonadotrophin; IBMX, 3-isobutyl-1-methylxanthine; MBP, myelin basic protein; MO, morpholino; MPF, maturation-promoting factor; PMSG, pregnant male serum gonadotrophin; PVA, polyvinyl alcohol; SCF, Skp1–Cul1–F box.

© The Rockefeller University Press $15.00
The Journal of Cell Biology, Vol. 176, No. 1, January 1, 2007 65–75
http://www.jcb.org/cgi/doi/10.1083/jcb.200607070

(Li and Nicklas, 1995; Cleveland et al., 2003). The proteins MAD2 and BubR1 complex with Cdc20 to ensure that the APC remains inactive until all chromosomes are bioriented on the spindle (Fang et al., 1998; Fang, 2002; Homer et al., 2005).

A more recently discovered APC inhibitor is early mitotic inhibitor 1 (Emi1; Reimann et al., 2001a,b; Reimann and Jackson, 2002). Depletion of Emi1 from mammalian cells results in an S-phase arrest as a result of the failure to accumulate S-phase activators, including cyclin A. In cycling *Xenopus laevis* extracts, the depletion of Emi1 arrests the extract before entry into mitosis as a result of a failure to accumulate cyclin B (Reimann et al., 2001a; Hsu et al., 2002). In prometaphase, Polo-like kinase–dependent phosphorylation of Emi1 targets it for destruction through the Skp1–Cul1–F-box (SCF) E3 ubiquitin ligase pathway (Hansen et al., 2004; Moshe et al., 2004). The F-box protein βTrCP is responsible for recruiting Emi1 to its SCF partners (SCF–βTrCP), triggering Emi1 degradation (Guardavaccaro et al., 2003; Margottin-Goguet et al., 2003). The inactivation of Emi1 in prometaphase is necessary to allow APC^{Cdc20} activation during mitosis, which is necessary to coordinate the destruction of securin and cyclin B.

Experiments conducted thus far address the role of Emi1 in meiosis II but have not focused on a role in meiosis I (Reimann and Jackson, 2002; Ohsumi et al., 2004; Paronetto et al., 2004; Shoji et al., 2006). However, there is evidence to indicate that Emi1 may play a role during meiosis I. A recent study shows that APC^{Cdh1} activity was found to be important for preventing the entry of prophase I–arrested mouse oocytes into the first meiotic division (Reis et al., 2006). This effect may be mediated by suppressing the levels of meiotic activators such as cyclin B1. This rather surprising finding provides a new potential role for APC regulation by Emi1 in meiosis I.

In this study, we investigate the role of Emi1 in meiosis I using exogenous GFP-hEmi1 and by depleting Emi1 from prophase I–arrested oocytes using morpholino (MO) oligonucleotides. We show that Emi1 is present in mouse oocytes and that its destruction is initiated immediately after GVBD. Microinjection of excess Emi1 accelerates entry into the first meiosis and arrests the oocyte at MI. The depletion of Emi1 delays entry into meiosis I and prevents normal MI spindle formation. Finally, we show that the effects of Emi1 depletion require Cdh1, thereby demonstrating that Emi1-dependent regulation of APC^{Cdh1} is essential for regulating prophase I arrest and progression through meiosis I.

Results

Emi1 is expressed in mouse oocytes

We first examined whether Emi1 was expressed in mouse oocytes. RT-PCR of mRNA extracted from 15 GV-stage oocytes generated a product of the expected molecular weight (218 bp). Control samples lacking reverse transcriptase failed to generate a PCR product (Fig. 1 A). In situ hybridization analysis of mouse ovaries reveals the wide-spread expression of Emi1, with the highest signal being present in oocytes and granulosa cells (Fig. 1 B). Negative controls show no signal arising from oocytes or granulosa cells (unpublished data). Western blotting analysis using an anti-Emi1 antibody revealed a band at the expected molecular mass of 49 kD (Fig. 1, C–F). To identify Emi1 in our Western blotting experiments, we used an Emi1 MO to deplete the protein. Emi1 MO and control MO were injected into GV-stage oocytes. Injected oocytes were maintained in 3-isobutyl-1-methylxanthine (IBMX)–mediated prophase I arrest for 24 h before being subjected to analysis by Western blotting

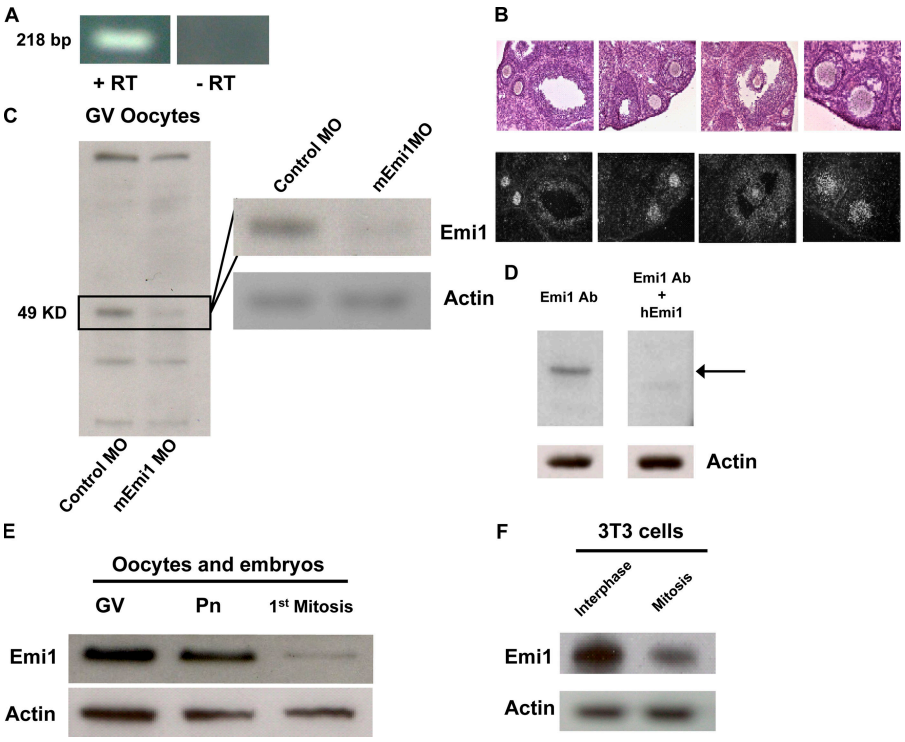

Figure 1. **Emi1 is expressed in GV-arrested oocytes.** (A–C and E) RT-PCR (15 oocytes; A), in situ hybridization (B), and Western blotting (200 oocytes/embryos; C and E) show the presence of Emi1 at the mRNA and protein level in GV-stage oocytes. (C) To identify the band corresponding to Emi1 in our Western blotting experiments, we depleted Emi1 from mouse oocytes by the use of a morpholino (MO) oligonucleotide targeted against mEmi1. A 49-kD band can be identified as Emi1 because it is present in oocytes injected with a control MO but absent from Emi1 MO–injected oocytes (three experiments). The loss of immunoreactivity corresponds to an 83% depletion of Emi1 in GV-stage oocytes injected with mEmi1 MO. (D) Further verification of the band corresponding to Emi1 was provided by an antigen block experiment in which the band is only present in the sample where the Gentaur Emi1 antibody is not neutralized by incubation with human Emi1 protein before blotting (two experiments). Arrow indicates Emi1. (E and F) One-cell embryos (E) and 3T3 cells (F) were arrested in metaphase with nocodazole (two experiments). The immunoreactive Emi1 shows an expected decrease in metaphase. Samples of 5 μg 3T3 cell lysates were used. Reprobing the blots with actin shows that loading is the same in the lanes examined. Pn, pronucleus stage.

(Fig. 1 C). Emi1 MO but not control MO resulted in the down-regulation of a 49-kD Emi1 band to ~17% of control levels (Fig. 1 C). The depletion of Emi1 appeared to be specific, as several cross-reactive bands did not show any change, and reprobing the blot for actin revealed that loading was similar in the two lanes. Furthermore, using hEmi1 as an antigen block, we were able to eliminate the Emi1 band on the blot (Fig. 1 D). This Emi1 band was also present in interphase pronucleate-stage embryos but was reduced in one-cell embryos arrested in mitosis using nocodazole (Fig. 1 E). This is consistent with the known cell cycle–dependent destruction of Emi1 in prometaphase (Reimann et al., 2001a; Margottin-Goguet et al., 2003). This was confirmed in 3T3 cells in the same conditions used for oocytes and embryos (Fig. 1 F).

The destruction of Emi1 occurs during oocyte maturation and is required for the MI→MII transition

The levels of Emi1 protein present during oocyte maturation were examined using Western analysis. At the GV stage, an immunoreactive protein was present. During maturation, the intensity of the band decreased to barely detectable levels in MI- and MII-stage oocytes (Fig. 2 A). This indicates that Emi1 is destroyed between GVBD and MI. Emi1 destruction may be necessary during maturation to permit an increase in APC activity and, thereby, the destruction of securin and cyclin B during the MI→MII transition. To test the requirement of Emi1 destruction, we used two independent approaches. First, we expressed GFP-hEmi1 during meiosis so as to maintain elevated levels of Emi1 during meiosis, and, second, we inhibited Emi1 destruction using βTrCPΔF. βTrCPΔF is a dominant-negative form of βTrCP, which binds to substrates such as Emi1 but not to the SCF ligase (Margottin-Goguet et al., 2003). In both experimental paradigms, the phenotype is the same: arrest at meiosis I with an intact spindle and condensed, aligned chromosomes (Fig. 2, B and C). Thus, Emi1 destruction is necessary during MI, presumably to allow the APC to become active once all other checkpoint requirements have been met.

Emi1 destruction is initiated immediately after GVBD and is SCF–βTrCP dependent

The loss of Emi1 immunoreactivity between the GV stage and MI suggests that Emi1 stability changes during oocyte maturation. In mitotic cells, Emi1 destruction is initiated in prophase and requires phosphorylation by Polo-like kinase 1 (Hansen et al., 2004; Moshe et al., 2004). To relate the timing of Emi1 destruction to meiotic progression, we asked whether Emi1 stability changed around the time of GVBD as oocytes make the transition from prophase to M phase. Oocytes were coinjected with a 70-kD rhodamine-dextran to provide an accurate timing of GVBD and with complementary RNA (cRNA) for GFP-hEmi1 to provide a measure of Emi1 stability. Imaging experiments revealed that before GVBD, Emi1 was stable and showed only a minor decrease in fluorescence (Fig. 3 A). The onset of GVBD was marked by an increase in rhodamine fluorescence in the region of the GV, and, within 5 min, an increase in the destruction of GFP-hEmi1 was detectable (Fig. 3 A). The time course of destruction of endogenous Emi1 was investigated using Western analysis of oocytes at the GV stage after GVBD and progressively through meiosis I (3, 6, and 9 h after release from IBMX). The data show that Emi1 is high in GV-stage oocytes and is reduced by 3 h after release from meiotic arrest (Fig. 3 B). Together, these data show that GVBD is tightly correlated with and may initiate the onset of Emi1 destruction.

To verify that Emi1 was being destroyed in oocytes by the established SCF–βTrCP-dependent pathway, GFP-hEmi1 stability was monitored in oocytes coinjected with the dominant-negative form of βTrCP (βTrCPΔF). The coinjection of βTrCPΔF resulted in a three- to fourfold decrease in the rate of Emi1 destruction after GVBD (Fig. 3, C and D).

Emi1 is sufficient to accelerate entry into the first meiosis

Because Emi1 is an APC inhibitor, it is likely to influence the levels of cyclin, which may alter the timing of progression through meiosis I. In experiments described in Fig. 2, we observed an apparent acceleration of GVBD in GFP-hEmi1–injected oocytes. This was confirmed by designing experiments in which GVBD was scored every 10–15 min in control and GFP-hEmi1–injected oocytes. GFP-hEmi1–injected oocytes underwent GVBD earlier than control GFP cRNA-injected oocytes (Fig. 4 A). Thus, after release from IBMX, 50% of GFP-hEmi1–injected oocytes had undergone GVBD at 45 min compared with 60 min in the control. Maximal rates of GVBD were achieved at 60 min in GFP-hEmi1–injected oocytes compared with 75 min in the controls (Fig. 4 A).

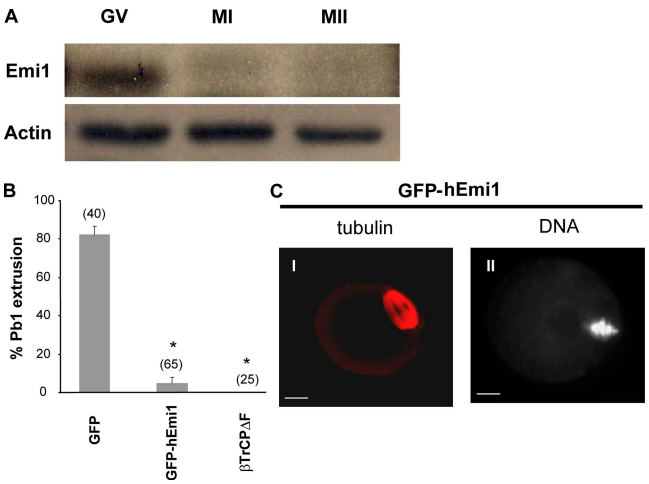

Figure 2. **Emi1 destruction is necessary for progression through meiosis I.** (A) Western blot analysis (200 oocytes/lane) shows that Emi1 immunoreactivity decreases between the GV stage and metaphase I (MI; 6 h after release from prophase arrest) and remains at low levels in metaphase II (three experiments). (B and C) GV-stage oocytes were injected with GFP-hEmi1 (three experiments) or βTrCP-ΔF (two experiments) cRNA, and polar body (Pb1) emission was scored. Maintaining Emi1 through meiosis I inhibits polar body extrusion. Labeling of tubulin with immunofluorescence showed that the GFP-hEmi1–injected oocytes were arrested at metaphase, as revealed by the presence of an intact MI spindle at the cortex (C, panel I) and aligned chromosomes (C, panel II; different oocyte than panel I). A similar phenotype is induced by βTrCP-ΔF. The number of oocytes assessed for each condition is given in parentheses. Error bars represent SD. *, $P < 0.0001$. Bars, 10 μm.

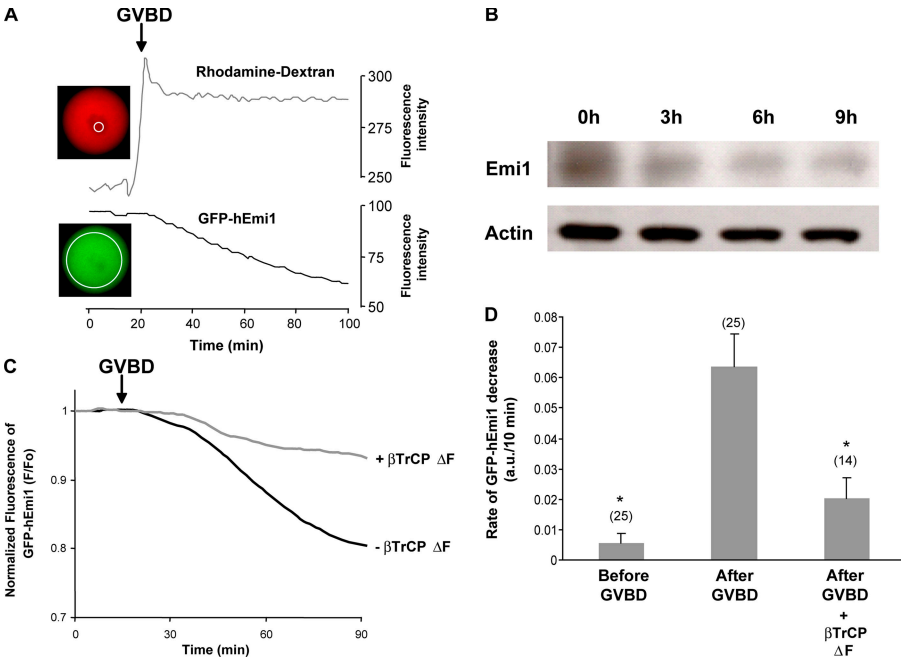

Figure 3. **Emi1 destruction is initiated at GVBD and is regulated by SCF–βTrCP.** (A) Fluorescence measurements of rhodamine-dextran and GFP-hEmi1 in the regions of interest (white circle) over the period of GVBD. The large increase in rhodamine fluorescence in the GV area marks GVBD. This is rapidly followed by an increase in the destruction of GFP-hEm1 (three experiments). (B) Endogenous Emi1 destruction early in meiosis I was determined by Western blotting and was found to occur by 3 h from release from prophase arrest. Time values correspond to time from the release from IBMX (150 oocytes; two experiments). (C) Records of GFP-hEmi1 in control oocytes and oocytes expressing βTrCP-ΔF. (D) GFP-hEmi1 levels are stabilized after GVBD by the presence of βTrCP-ΔF (two experiments). The number of oocytes is given in parentheses. Time at 0 min corresponds to the release of GV-stage oocytes from IBMX. Error bars represent SD. *, $P < 0.0001$.

We next examined whether the expression of GFP-hEmi1 could override cAMP-mediated prophase arrest. Oocytes were incubated in 30 μM IBMX, which allows ∼10% of GFP cRNA-injected oocytes to escape meiotic arrest during incubation for 20 h (Fig. 4 B). In these conditions, the rate of GVBD after the injection of GFP-hEmi1 was increased to 70% (Fig. 4 B). These data show that Emi1 has a dramatic effect on entry into the first meiotic division, presumably as a result of its ability to inhibit the APC.

Next, we examined whether Emi1 regulates APC activity in GV-stage oocytes by monitoring the rate of destruction of the APC substrate cyclin B1–GFP in IBMX-arrested oocytes injected with a cRNA for myc-hEmi1. The injected cyclin B1–GFP protein was degraded slowly in GV-stage oocytes, with ∼10% of the signal being depleted over 3 h (Fig. 4 C). In oocytes previously injected with myc-Emi1, the rate of cyclin B1–GFP destruction was attenuated such that only 3% of the cyclin B1–GFP was destroyed in the same period. These experiments show that the APC is active in prophase-arrested oocytes and that its inhibition by Emi1 is sufficient to accelerate the resumption of meiosis.

Depletion of Emi1 delays entry into the first meiotic division

To understand the physiological role of Emi1 in meiosis I, we next examined the timing of GVBD in Emi1 MO–injected oocytes.

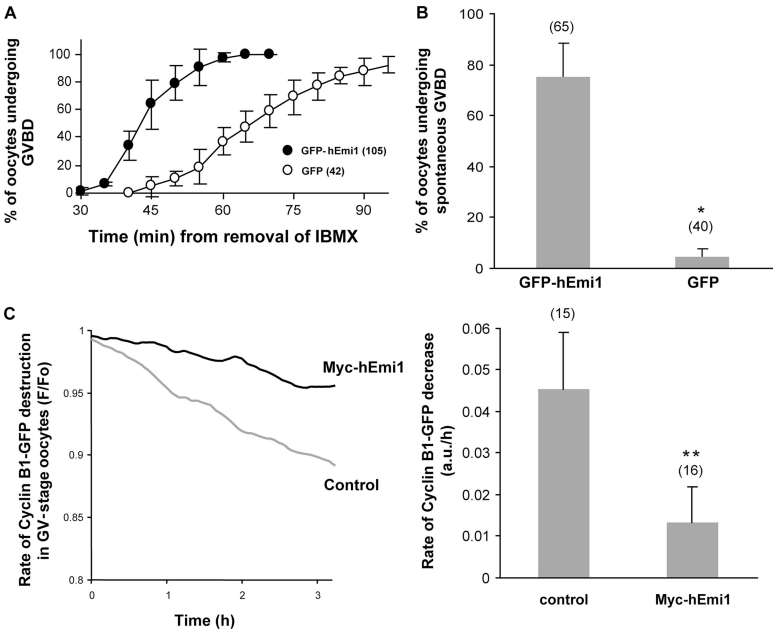

Figure 4. **Emi1 accelerates GVBD and stabilizes cyclin B in mouse oocytes.** (A) Timing of GVBD in oocytes injected with GFP-hEmi1 cRNA 12–14 h before release from 200 μM IBMX (time 0). Control oocytes were injected with GFP cRNA and treated identically to GFP-hEmi1–containing oocytes. Note the acceleration of GVBD by GFP-hEmi1. Data are from four experiments. (B) Oocytes were injected with GFP-hEmi1 or GFP (controls) and incubated for 24 h in 30 μM IBMX. GFP-hEmi1 overrides IBMX-mediated arrest. Data are from three experiments. (C) Representative traces showing the rate of cyclin B1–GFP destruction in control oocytes and in oocytes coinjected with cRNA for myc-hEmi1. Oocytes were maintained in 200 μM IBMX for the duration of the experiment. In the right panel, the rate of cyclin B1 destruction is quantified. Data are from two experiments. The number of oocytes assessed for each condition is given in parentheses. Error bars represent SD. *, $P < 0.0001$; **, $P < 0.01$.

As shown in Fig. 1 C, Emi1 MO–injected oocytes are depleted of ~83% of the endogenous Emi1 after 24 h of culture. If Emi1-dependent regulation of the APC plays a role in the timing of meiosis entry, the depletion of Emi1 would be expected to increase APC activity and maintain meiotic arrest. The results in Fig. 5 A show that consistent with this hypothesis, the depletion of Emi1 delays GVBD such that 50% of control oocytes undergo GVBD at 65 min after release from IBMX compared with 110 min in Emi1 MO–treated oocytes (Fig. 5 A). This delay was rescued by the coinjection of cRNA encoding GFP-hEmi1, suggesting that effects are specific to the depletion of Emi1.

The depletion of Emi1 may prevent the accumulation of APC substrates such as cyclin B1. This would be expected to result in a delay in MPF activation. To test this possibility, we measured H1 kinase activity in Emi1 MO–injected oocytes (Fig. 5 B). H1 kinase activity in control oocytes increased 2.5-fold in the first hour and fourfold over 3 h. Emi1 MO treatment delayed H1 kinase activity such that no increase was apparent after 1 h, reaching a maximum twofold increase at 2 h (Fig. 5 B). This increase was apparently sufficient to induce GVBD, but with much delayed timing.

To confirm that Emi1 MO caused cyclin B1 instability in GV-stage oocytes, we monitored the rate of cyclin B1–GFP accumulation after microinjection with cyclin B1 cRNA in oocytes injected with control and Emi1 MOs. Emi1 MO–injected oocytes accumulated cyclin B1–GFP at a rate three- to fourfold slower than oocytes injected with control MO (Fig. 5 C). The decrease in cyclin B1–GFP fluorescence was caused by destruction because nondestructible cyclin $B1^{\Delta 90}$-GFP was accumulated at a rate twofold greater than that of controls (Fig. 5 C). This further illustrates that cyclin B1–GFP is undergoing destruction in GV-stage oocytes.

Emi1 is necessary for spindle formation and progression through MI

Continued cyclin synthesis and increasing MPF activity are required for progression through MI (Tay et al., 2000; Ledan et al., 2001). The decrease in MPF activity described in Emi1-depleted oocytes raised the possibility that Emi1 may be needed for the cyclin B accumulation necessary for progression through the first meiotic division. We tested this hypothesis by examining Emi1-depleted oocytes for normal MI spindle formation

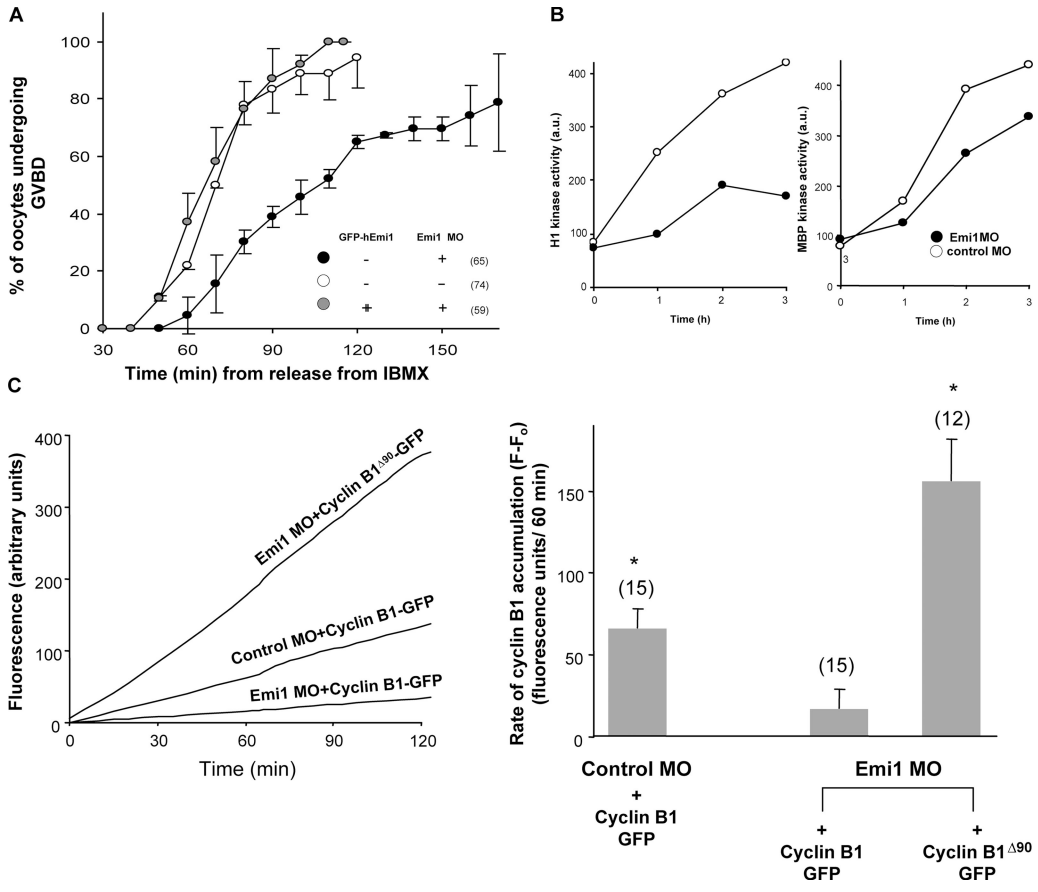

Figure 5. **Depletion of Emi1 leads to premature APC activation and subsequent delay in GVBD.** (A) The timing of GVBD is delayed in oocytes depleted of Emi1 using Emi1 MO. Coinjection of GFP-hEmi1 with Emi1 MO reverses the delay. The experiment was repeated four times. (B) H1 kinase (MPF) and MBP kinase (MAPK) activities in control oocytes and Emi1-depleted oocytes. Representative of two independent experiments. (C) Representative traces (left) and quantification (right) of the effect of Emi1 depletion on the accumulation of cyclin B1–GFP. Emi1-depleted oocytes have a much reduced ability to accumulate cyclin B1–GFP. Nondestructible cyclin $B1^{\Delta 90}$-GFP accumulates at a rate five- to sixfold more than cyclin B1–GFP, showing that the effects of Emi1 MO are caused by cyclin B1 stability rather than translation. Data were obtained from two experiments. Time 0 corresponds to 15 min after cRNA injection. The number of oocytes assessed for each condition is given in parentheses. Error bars represent SD. *, $P < 0.0001$.

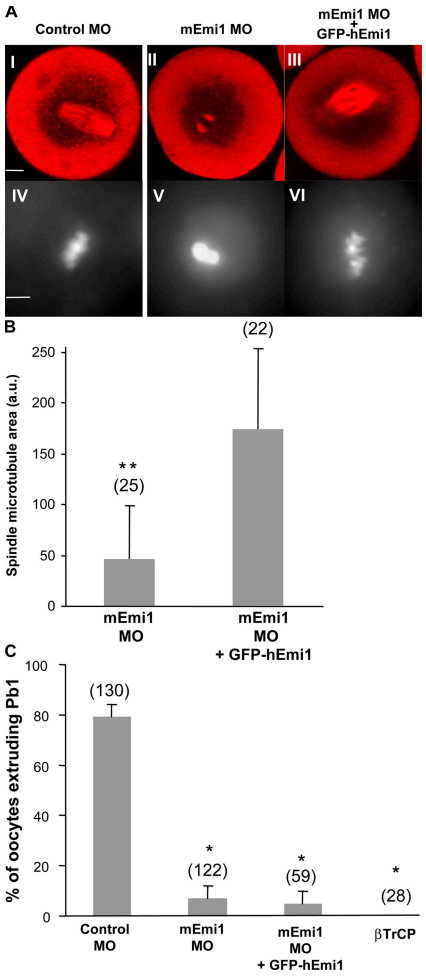

Figure 6. **Emi1 is important for spindle formation.** (A) Control MO–injected oocytes were released from IBMX and fixed for immunocytochemistry 7 h later, at the time when a fully developed spindle is formed (panel I), and chromosomes are aligned at the metaphase plate (panel IV). Emi1 MO–injected oocytes were fixed 16–18 h after release from IBMX, by which time they were arrested (C). These oocytes show only the most rudimentary of spindle structures (panel II), whereas their chromosomes decondensed, forming clumps of chromatin (panel V). Coinjection of Emi1 MO and GFP-hEmi1 cRNA partially reverses the MO effect (panels III and VI). Bars, 10 μm. (B) The extent of rescue was determined by measuring the microtubular area of the oocytes. Microtubule polymerization was three to four times stronger in GFP-hEmi1 + Emi1 MO–injected oocytes than in oocytes injected with Emi1 MO alone (oocytes from both groups were fixed and analyzed 16–18 h after release from IBMX; two experiments). (C) The absence of a normal spindle leads to the inhibition of polar body (Pb1) extrusion in Emi1 MO–injected oocytes (five experiments). Inhibition is also observed in oocytes coinjected with Emi1 MO and GFP-hEmi1 cRNA because the MO phenotype is not totally recovered in these oocytes (three experiments). βTrCP cRNA expression in oocytes mimics the Emi1 MO effect, causing the inhibition of polar body extrusion (two experiments). The number of oocytes assessed for each condition is given in parentheses. Error bars represent SD. *, $P < 0.0001$; **, $P < 0.005$.

and the ability to extrude the first polar body. Emi1-depleted and control oocytes were matured and fixed, and their spindles and chromosomes were examined using confocal microscopy. Control MO–injected oocytes progress through MI and extrude the first polar body, so, for the purpose of comparison, an image of a control oocyte at MI is shown 7–8 h after release from IBMX (Fig. 6 A, I). In contrast to the normal spindles that form in controls, Emi1 MO–treated oocytes showed only the most rudimentary of spindle structures even after prolonged incubation for 12–24 h (Fig. 6, A and B). The extent of microtubule polymerization was limited and was often restricted to two small spindle poles (Fig. 6, A and B). Staining of chromatin in the Emi1-depleted oocytes revealed that the chromatin formed a condensed clump associated with the putative spindle structure. Individual chromosomes could not be resolved (Fig. 6 A). This phenotype is also observed after the expression of βTrCP in oocytes, which was used as an indirect way to verify that the Emi1 MO effect is specific to Emi1 depletion (Fig. 6 C). This effect was further confirmed to be specific for the effects of Emi1 depletion because it was partially reversed using GFP-hEmi1 (Fig. 6, A and B). Coinjection of GFP-hEmi1 cRNA and Emi1 MO resulted in the presence of spindlelike structures and an increased microtubular area after release from cAMP-mediated arrest compared with Emi1-depleted oocytes (Fig. 6, A and B). We confirmed in a separate series of experiments that Emi1 MO results in inhibition of the MI→MII transition (Fig. 6 C). This effect was not reversed by exogenous GFP-hEmi1, but this is not surprising given that excess Emi1 also causes arrest at MI (Fig. 2 B).

The effects of Emi1 depletion on meiosis I are mediated by APC^{Cdh1}

To test the hypothesis that the effects of Emi1 on GVBD and polar body extrusion are mediated by APC^{Cdh1}, we coinjected Emi1 MO and Cdh1 MO. If Cdh1 is the downstream effector of Emi1, the depletion of Emi1 would be expected to be without effect in Cdh1-depleted oocytes. Oocytes were injected with control, Emi1, or a previously characterized Cdh1 MO (Reis et al., 2006) or were coinjected with Emi1 and Cdh1 MO. The oocytes were then incubated in 30 μM IBMX, and GVBD and polar body extrusion were examined at 24 and 48 h.

As expected from previous experiments, the control and Emi1 MO–injected oocytes remained arrested at the GV stage throughout the 48-h incubation (Fig. 7 A). Consistent with a previous study (Reis et al., 2006), oocytes injected with Cdh1 MO alone underwent GVBD such that ∼40 and 80% of oocytes underwent GVBD at 24 and 48 h, respectively (Fig. 7 A). Oocytes coinjected with Emi1 MO and Cdh1 MO underwent GVBD at rates similar to those receiving Cdh1 MO alone. This indicates that Emi1 acts in the same pathway as Cdh1 in regulating meiotic arrest.

It was noted that most oocytes coinjected with Emi1 MO and Cdh1 MO progressed beyond GVBD and went on to extrude the first polar body by the 48-h time point (Fig. 7 B). This is consistent with the observation that several of these oocytes displayed apparently normal MI spindles with aligned chromosomes at the 24-h time point (unpublished data). To confirm that controls progress to MI and that oocytes injected with Emi1 MO alone display prometaphase arrest, as shown in Fig. 6, a proportion of these oocytes was released from IBMX after 24 h and scored for polar body extrusion at 48 h (Fig. 7 B). The results confirm that Emi1MO–injected oocytes arrest in prometaphase and that this arrest is reversed in the absence of Cdh1.

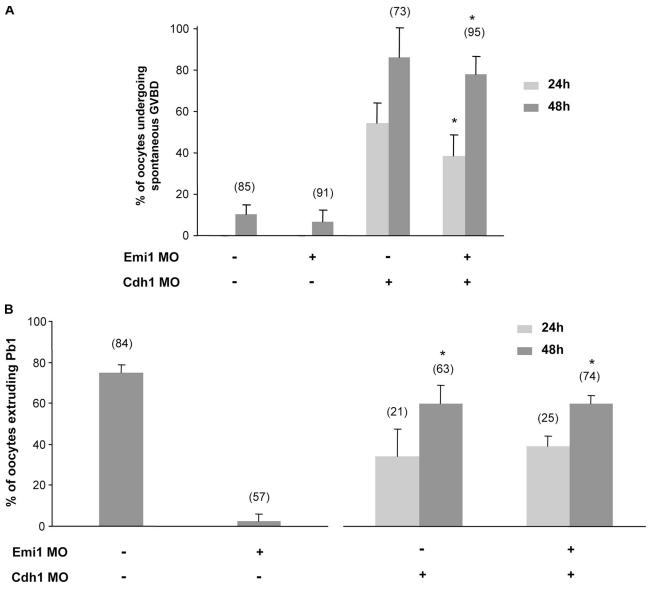

Figure 7. **The effects of Emi1 in meiosis I are mediated by APC^{Cdh1}.** (A and B) Emi1 depletion has no effect on GVBD in Cdh1-depleted oocytes (A), and depletion of Cdh1 reverses the effects of Emi1 MO on polar body (Pb1) extrusion (B). GV-stage oocytes were injected with control MO, Emi1 MO, or Cdh1 MO or were coinjected with Emi1 MO and Cdh1 MO. Oocytes were incubated in medium containing 30 μM IBMX, and the rate of GVBD and polar body extrusion was recorded 24 and 48 h after injection. (B, left) At 24 h after injection, a proportion of the control MO and Emi1 MO–injected oocytes were released from IBMX to confirm that the Emi1 MO was functioning to inhibit polar body extrusion as described in Fig. 6. (A) Emi1 MO does not maintain prophase I arrest in oocytes coinjected with Cdh1 MO. (B) Similarly, the early prometaphase arrest and resultant inhibition of polar body extrusion induced by Emi1 MO was reversed by the codepletion of Cdh1. The graph shows the proportion of GVBD-stage oocytes that extruded the first polar body at 24 and 48 h after injection. The number of oocytes assessed for each condition is given in parentheses. Error bars represent SD. *, $P < 0.0001$.

Discussion

Emi1 is a relatively new player in the family of cell cycle proteins that have a critical role in regulating the APC. It is known to restrain APC activity so as to allow the accumulation of cyclin A and cyclin B in S and G2/M phases of the mitotic cell cycle (Reimann et al., 2001a; Hsu et al., 2002). In this study, we describe the first definitive evidence of a role for Emi1 acting via APC^{Cdh1} in regulating the timing of entry into meiosis I and progression through the first meiotic division.

Emi1 in meiosis I: balancing prophase I arrest through APC^{Cdh1}

The importance of Emi1 in balancing meiotic arrest at prophase I is shown by the opposing effects of exogenous Emi1 and the depletion of Emi1 on the timing of GVBD. Entry into the first meiotic division is delayed or inhibited by the depletion of Emi1 and is accelerated by excess Emi1. The APC is apparently the target of Emi1 in mediating entry into meiosis I because exogenous Emi1 leads to an increase in the stability of the APC substrate cyclin B1, whereas Emi1 depletion leads to cyclin B1–GFP instability. This increase in cyclin instability likely explains the much-attenuated increase in MPF activity during the first 3 h of the meiotic progression of Emi1-depleted oocytes. The recent observation that APC^{Cdh1} is necessary for maintaining prophase I arrest in mouse oocytes (Reis et al., 2006) provides a strong lead as to the target of Emi1 for its role in regulating entry into meiosis I. Our results show that Emi1 MO is without effect in oocytes that are codepleted of Cdh1, indicating that the Emi1-dependent inhibition of APC^{Cdh1} is important in the control of entry into meiosis I. Thus, prophase I arrest is critically poised by the competing actions of APC^{Cdh1} and Emi1. The physiological regulation of Emi1-APC^{Cdh1} that allows for a timely initiation of meiotic maturation is a topic for future investigation.

Our observations may have wider implications for the role of Emi1 in the mitotic cell cycle. In mammalian somatic cells, Emi1 has been shown to inhibit APC^{Cdh1} to allow the accumulation of S-phase regulators, including cyclin A (Hsu et al., 2002). In cycling *Xenopus* extracts, the depletion of Emi1 leads to a failure of nuclei to enter metaphase, an effect attributed to the unbridled activity of APC^{Cdc20} and a failure to accumulate cyclin B (Reimann et al., 2001a). The mouse oocyte has provided an opportune model system in which the cell cycle is arrested at the G2→M transition. As a result, the effects of Emi1 depletion at the G2→M transition have been elucidated using highly specific MO-based technology in which results can be interpreted independently of the effects of Emi1 on S phase. Indeed, this role in prophase I arrest in mammalian meiosis is entirely consistent with the effects of the *Drosophila melanogaster* Emi1 homologue Rca1, which, when mutated, results in G2 arrest (Grosskortenhaus and Sprenger, 2002). It will be important to determine whether entry into mitosis is controlled by Emi1-APC^{Cdh1} as it is at entry into meiosis I.

Recent studies have investigated the role of Emi1 in oocyte maturation (Paronetto et al., 2004; Shoji et al., 2006), but a role for Emi1 in entry into the first meiotic division has not been revealed. This is likely a result of the fact that Emi1 was considered to be an excellent candidate for CSF and that the first experiments targeted MII arrest (Paronetto et al., 2004; Shoji et al., 2006). In experiments on MII oocytes, we found that exogenous Emi1 delayed egg activation but that depletion only sensitized eggs to activation rather than caused egg activation (unpublished data). Furthermore, we have shown by Western analysis that the level of Emi1 protein decreases as oocytes enter the first meiotic division. This is inconsistent with a role in MII arrest but entirely in line with a role in S phase and prophase (Reimann et al., 2001a; Margottin-Goguet et al., 2003). In *Xenopus* oocytes, an Emi1 antibody inhibits GVBD (Tung and Jackson, 2005), but these authors raised concerns about cross-reactivity of the antibody with additional Emi1-related proteins, resulting in some uncertainty as to which Emi1 orthologue was responsible. Assuming Emi1 was indeed the target in *Xenopus* oocytes, this study, together with the present data, suggests a conserved role amongst vertebrates for Emi1 in regulating prophase I arrest.

Emi1 is required for formation of the MI spindle

Depletion of Emi1 from GV-stage oocytes delays GVBD, but a more dramatic effect is seen further downstream, where it

prevents formation of the MI spindle. As a result, extrusion of the first polar body does not take place. The small or absent spindles and partially condensed chromatin is consistent with an arrest early in prometaphase I. We examined the localization of Mad2 using immunofluorescence in these arrested oocytes and found that Mad2 was surrounding the chromatin but was not localized to kinetochores (unpublished data), which is consistent with an early prometaphase arrest (Wassmann et al., 2003). A likely explanation for the arrest at this stage is the failure of Emi1-depleted oocytes to accumulate cyclin B1, resulting in the muted (threefold) activation of MPF compared with controls. It is already established that an increase in MPF activation driven by the continued synthesis of cyclin B1 is necessary for spindle formation and progression through MI (Polanski et al., 1998; Ledan et al., 2001; Marangos and Carroll, 2004b; Brunet and Maro, 2005). Presumably, the increased APC activity in the absence of Emi1 is sufficient to prevent MPF from reaching the critical levels required for spindle formation. This conclusion is further supported by the finding that the spindle defect and inhibition of polar body extrusion are reversed in Emi1- and Cdh1-depleted oocytes. In addition to the effects on prophase I arrest, the suppression of APC^{Cdh1} by Emi1 is clearly necessary for progression from prometaphase to metaphase of meiosis I.

In previous studies in mouse oocytes, the evidence for a role of Emi1 in meiosis I is contradictory (Paronetto et al., 2004; Shoji et al., 2006). These differences may be caused by problems with specificity and validation of the siRNA approaches (Shoji et al., 2006). In both cases, the studies were focused on a role in metaphase II. As such, the siRNA was injected just before release from meiotic arrest and would not have provided sufficient time to deplete the levels of Emi1 protein. In the present study, we found it necessary to inject Emi1 MO 20–24 h before release from IBMX to achieve a >80% reduction in protein and a consistent phenotype. The partial reversal of the spindle defect using cRNA for Emi1 and the requirement of Cdh1 to induce the phenotype are important controls pointing to the specificity of the MO approach used in this study.

Emi1 destruction is necessary for the MI→MII transition

The requirement for Emi1 to be destroyed is shown by the injection of excess Emi1, which results in a strong block at MI with an apparently normal MI spindle. This phenotype is mimicked by the injection of βTrCPΔF, which inhibits the destruction of SCF substrates, including Emi1 (Guardavaccaro et al., 2003; Margottin-Goguet et al., 2003; and this study). Persistent or elevated levels of Emi1 during meiosis I most likely lead to an inhibition of the APC (probably APC^{Cdc20}) with the result that the spindle develops normally but cannot proceed further in the absence of APC^{Cdc20}-dependent cyclin B destruction. This requirement for APC activity is in agreement with the finding that APC-dependent securin destruction is necessary for homologue disjunction at MI in mouse oocytes (Herbert et al., 2003; Terret et al., 2003), although APC activity is apparently unnecessary for the MI→MII transition in *Xenopus* (Peter et al., 2001).

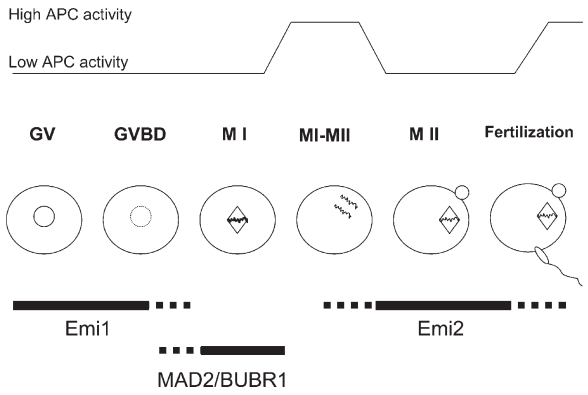

Figure 8. **Regulation of the APC in meiosis.** Low levels of APC activity are partly responsible for prophase I arrest. After release from the arrest and during the early stages of oocyte maturation, Emi1 ensures that APC activity is maintained at low levels, allowing cyclin B accumulation and MPF activation. After Emi1 destruction, this role is passed to spindle assembly checkpoint proteins such as MAD2 and BUBR1. During the MI→MII transition, cyclin B and securin destruction depend on APC activation, which is provided by the silencing of the spindle assembly checkpoint. The expression of Emi2 during extrusion of the first polar body will lead to APC inhibition and CSF arrest in metaphase II, pending fertilization.

Our data show that Emi1 is largely destroyed between the GV and MI stages. Precise timing of the onset of Emi1 destruction was investigated using GFP-hEmi1. These experiments revealed that Emi1 destruction starts within 5–10 min of the GV becoming permeable to large molecular weight dextran molecules. The significance of the timing relative to GVBD may be coincidence because GVBD rapidly follows MPF activation, but it may indicate a role for the necessity of nuclear factors in initiating Emi1 destruction. βTrCP1 is a nuclear protein, whereas its homologue βTrCP2 is cytoplasmic (Davis et al., 2002). In somatic cells, it is thought that Emi1 is bound by βTrCP1/βTrCP2 heterodimers before being ubiquitinated by the SCF ligase (Guardavaccaro et al., 2003). This unusual feature of Emi1 as a βTrCP substrate may provide a fail-safe mechanism to prevent the premature destruction of Emi1 before MPF is activated sufficiently to induce nuclear envelope breakdown.

From Emi1 to Emi2: cyclin B stability during oocyte maturation

Regulation of cyclin stability is important for arresting the meiotic cell cycle at two stages. First, this is important in prophase arrest, where the Emi1-dependent inhibition of APC^{Cdh1} increases cyclin B accumulation and controls entry into and progression through meiosis I. Emi1 destruction is stimulated after GVBD, marking the end of its main role in meiosis I. Arrest at metaphase II has been recently attributed to the Emi1 orthologue Emi2 (Liu and Maller, 2005; Rauh et al., 2005; Tung et al., 2005; Hansen et al., 2006; Madgwick et al., 2006; Shoji et al., 2006). Thus, Emi1 plays an important role in timing of the early stages of meiotic maturation before handing over to spindle assembly checkpoint proteins in prometaphase I and finally to Emi2 for controlling cyclin stability and arrest at MII (Fig. 8).

Materials and methods

Oocyte and embryo collection

GV-stage oocytes were retrieved from the ovaries of 21–24-d-old female MF1 mice 48 h after the administration of 7 IU of pregnant male serum gonadotrophin (PMSG; Intervet) by intraperitoneal injection. Ovaries were released into warmed M2 (Sigma-Aldrich) supplemented with 200 μM IBMX (Sigma-Aldrich) to prevent GVBD and were maintained at 37°C. For oocyte maturation experiments, GV-stage oocytes were washed three times and transferred to M16 at 37°C in an atmosphere of 5% CO_2 in air. To recover mature (MII) oocytes, human chorionic gonadotrophin (hCG; Intervet) was administered 48–54 h after PMSG. Oviducts were removed 14–16 h after hCG. Cumulus masses were released into M2, and cumulus cells were removed by a brief incubation in M2 containing 300 μg/ml hyalauronidase (embryo-tested grade; Sigma-Aldrich). For the recovery of pronucleate embryos, female mice were mated with males at the time of hCG administration. The embryos were recovered from the oviduct in Hepes-buffered KSOM (Lawitts and Biggers, 1993) 27–28 h after hCG and mating. Embryos that were not immediately used were transferred to KSOM at 37°C in an atmosphere of 5% CO_2 in air.

Microinjection

Oocytes were pressure injected using a micropipette and Narishige manipulators mounted on an inverted microscope (DM IRB; Leica). Oocytes were placed in a drop of M2 containing IBMX covered with mineral oil to prevent evaporation. Cells were immobilized with a holding pipette while the injection pipette was pushed through the zona pellucida until making contact with the oocyte plasma membrane. A brief overcompensation of negative capacitance caused the pipette tip to penetrate the cell. Microinjection was performed using a fixed pressure pulse through a picopump (World Precision Instruments). Injection volumes were estimated at 2–5% of total cell volume by cytoplasmic displacement. The oocyte volume is ∼250 pl. After microinjection, the oocytes were removed in fresh drops of M2 + IBMX under oil and allowed to recover for a few minutes before any further manipulation.

Constructs and MO oligonucleotides

Human Emi1 was cloned into pCS2 + myc5 as described previously (Reimann et al., 2001a) and pCS2-eGFP-c1 (CLONTECH Laboratories, Inc.). pCS2-GFP was a gift from M.W. Klymkowsky (Colorado University, Boulder, CO). βTrCP and βTrCPΔF were cloned in pCS2 + HA (Margottin-Goguet et al., 2003). pMDL2–cyclin B1–GFP and pMDL2–cyclin $B1^{\Delta 90}$-GFP were gifts from M. Herbert (University of Newcastle, Newcastle, United Kingdom; Herbert et al., 2003). cRNAs encoding each of these constructs were made in vitro using the mMESSAGE mMACHINE kit (Ambion). The cRNAs were polyadenylated, purified, and dissolved in nuclease-free water to a concentration of ∼1 μg/μl before microinjection into GV-stage oocytes. For Emi1 knockdown in mouse oocytes, mEmi1 MO 5′-CGGGACAAGAAAGACAATGTTACTT-3′ (Gene Tools, LLC) was used at a concentration of 1.5 mM. For Cdh1 knockdown, we used an already characterized cdh1 MO (5′-CCTTCGCTCATAGTCCTGGTCCATG-3′; Reis et al., 2006). To control for possible nonspecific effects of the MOs, a control MO was also used (5′-CCTCTTACCTCATTACAATTTATA-3′).

RT-PCR

15 GV-stage oocytes were collected in 9 μl of nuclease-free water. After incubation with 2 U DNase I at 37°C for 30 min, the samples were subjected to oligonucleotide (dT)-primed first-strand cDNA synthesis in 20 μl by using the RETROscript kit (Ambion). The entire reaction was then used for PCR amplification with Deep Vent DNA polymerase (New England Biolabs, Inc.) for 35 cycles. The primers used for amplifying a 218-bp-long mouse Emi1 sequence were 5′-GTGGAGGTGGCAAAGACATT-3′ and 5′-GGCAAAGGACCCACTTTAC-3′. The reaction was accompanied by a negative (minus RT enzyme) control, and the experiment was repeated three times.

In situ hybridization

Ovaries of PMSG-primed mice were fixed in 4% PFA for 6 h followed by incubation in 0.5 M sucrose in PBS overnight at 4°C. The ovaries were embedded in optimal cutting temperature (Tissue-Tek), sectioned at 10 μm, and mounted on Superfrost slides (Fisher Scientific). The mouse Emi1 cDNA was subcloned into the pGEM3zf vector, linearized, and transcribed to synthesize ^{35}S-labeled RNA probes. Hybridization mixtures with antisense and sense RNA probes were added to the slide and incubated overnight at 50°C. Post hybridization washes consisted of RNaseA treatment and decreasing concentrations of SSC washes. Hybridized slides were then dehydrated and dried. Slides were dipped into NTB2 emulsion (Kodak), exposed for 2 d, developed photographically, and counterstained with Gill's hematoxylin and eosin Y (0.5% wt/vol in ethanol). After counterstaining, tissues were cleared with xylene, mounted with Permount, visualized, and photographed with a camera (AxioCam; Carl Zeiss MicroImaging, Inc.).

Cell culture

3T3 cells were grown in DME supplemented with 10% FBS (Invitrogen). DMSO or 10 μM nocodazole/DMSO was added in subconfluent monolayers that were harvested 48 h later, lysed (50 mM Hepes, pH 7.5, 75 mM NaCl, 10 mM glycerophosphate, 2 mM EGTA, 15 mM $MgCl_2$, 0.1 mM sodium orthovanadate, 1 mM DTT, 0.5% Triton X-100, and protease inhibitor cocktail [Sigma-Aldrich]), and incubated for 10 min on ice. Lysates corresponding to interphase (DMSO) or mitosis (nocodazole/DMSO) were centrifuged for 10 min at 10,000 *g* and 4°C. Protein concentration was determined using a protein assay kit (Bio-Rad Laboratories) according to the manufacturer's instructions. 5 μg of lysate was loaded onto gels for Western blotting.

Western blotting

Oocytes (200 oocytes/sample) were washed in PBS/polyvinyl alcohol (PVA) and frozen in SDS sample buffer (Laemmli, 1970). Proteins were separated on 4–12% NuPAGE gels (Invitrogen) and transferred to polyvinylidene fluoride Immobilon-P membranes (Millipore) using the XL II Blot Module (Invitrogen). The membranes were saturated with 5% nonfat dry milk in PBS containing 0.1% Tween 20 for 1 h at room temperature and were incubated with the primary antibodies overnight at 4°C. Three antibodies were used for Western blot analysis of Emi1. 1 μg/ml rabbit polyclonal (Gentaur), a mouse monoclonal (Zymed Laboratories), and 1 μg/ml of an affinity-purified rabbit polyclonal antibody were raised against a bacterially produced myelin basic protein (MBP)−mEmi1 fusion protein. Rabbit polyclonal antibodies were affinity purified with mEmi1 fused to GST. All antibodies provide similar results. For clarity, we have presented data obtained using the Gentaur antibody. Antigen block was performed using the Gentaur antibody by preincubation for 1 h at room temperature with a threefold molar excess of human Emi1-MBP. For the detection of actin, we used 1 μg/ml of a mouse monoclonal antiactin antibody (Chemicon). Secondary IgGs conjugated to 0.05 μM HRP (goat anti–rabbit IgG or mouse IgG; Sigma-Aldrich) were incubated with the membranes for 30 min at room temperature. Immunostained bands were detected by chemiluminescence (Pierce Chemical Co.).

Kinase assays

CDK1–cyclin B activity and MAPK activity were measured by their ability to phosphorylate histone H1 and MBP in vitro (H1 and MBP kinase assay), respectively, as previously described in detail (Marangos et al., 2003). Eight oocytes in 2 μl M2 were transferred in 3 μl of storing solution and immediately frozen on dry ice. The samples were diluted twice by the addition of concentrated kinase buffer (Marangos et al., 2003). The samples were then incubated at 37°C for 30 min and were analyzed by SDS-PAGE (as for Western blotting) followed by autoradiography. The autoradiographs were imaged using the phosphorimager system (Bas-100; Fuji) and analyzed with TINA 2.0 software.

Purified proteins

A baculovirus-based expression system was used to obtain recombinant human cyclin B1–GFP at a concentration of 2 mg/ml as described previously (Marangos and Carroll, 2004a). Sf9 insect cells infected with the baculovirus encoding $His(6)^{-}$ cyclin B1–GFP were a gift from J. Pines (Gurdon Institute, University of Cambridge, Cambridge, United Kingdom).

Immunofluorescence

Oocytes were fixed in freshly prepared 4% PFA (in PBS, pH 7.4, 1 mg/ml PVA) for 20 min, washed in PBS/PVA, and permeabilized in 0.1% Triton X-100 for 15 min. The cells were then incubated in blocking buffer (PBS, 3% BSA, and 10% normal goat serum) for 2 h at RT and in 5 μg/ml of a mouse anti–α-tubulin antibody (Abcam) in blocking buffer at 4°C overnight. The cells were incubated with 5 μg/ml of an AlexaFluor555-conjugated goat polyclonal anti–mouse IgG secondary antibody (Invitrogen) for 2 h at RT followed by incubation with 2 μM Hoechst 33342 to label the DNA. The immunostaining was visualized using a confocal microscope (LSM510 META; Carl Zeiss MicroImaging, Inc.). To ensure that comparisons of immunofluorescence could be made between treatment groups or developmental stages, the different samples were scanned and viewed with identical settings.

Imaging

For conventional microscopy, oocytes were placed in a drop of M2 medium under oil in a chamber and placed on a microscope (Axiovert; Carl Zeiss MicroImaging, Inc.). Cyclin B1–GFP and GFP-hEmi1 were imaged using a FITC filter set (450–490-nm excitation band-pass filter, 510-nm dichroic mirror, and 505–520-nm band-pass filter for emission). Fluorescence was collected through a 20× NA 0.75 objective. For simultaneous imaging of GFP and rhodamine-dextran, the fluorophores were excited through a monochromator (Oolychrome II; Till Photonics), which was used to select excitation wavelengths of 488 and 550 nm. A triple band-pass (DAPI/FITC/TRITC) dichroic mirror was used, and emitted fluorescence was collected through a 450–490-nm band-pass filter for GFP and a 600-nm-long pass filter for rhodamine. The emitted light from all of the fluorochromes was collected using a cooled CCD camera (MicroMax; Princeton Scientific Instruments). In all imaging experiments using conventional microscopy, data were collected and analyzed using Metafluor and MetaMorph software (Universal Imaging Corp.).

A confocal microscope (LSM510; Carl Zeiss MicroImaging, Inc.) was used for the monitoring of spindles and chromosomes in the immunolocalization experiments. A 40× NA 1.3 oil immersion lens (Carl Zeiss MicroImaging, Inc.) was used. Excitation of AlexaFluor555 was provided by the 543-nm laser line of a helion-neon laser, with the laser power set at 1% of maximum. Fluorescence was collected using a 560–615-nm band-pass emission filter. For imaging Hoechst, confocal images were obtained by exciting with the 351-nm laser line of a UV laser, and emission was collected through a 435–485-nm band-pass filter. For all confocal imaging experiments, a pinhole of 2.22 Airy U was used, giving a calculated optical slice of 3.5 μm. The images were analyzed using MetaMorph software.

We thank Mary Herbert for cyclin B1Δ90 and Katja Wassmann (Université Pierre et Marie Curie, Paris, France). for anti-Mad2 antibody.

This work was supported by a Medical Research Council grant to J. Carroll. E.W. Verschuren is funded by a Damon Runyon Cancer Research Foundation Fellowship (grant DRG-1811-04).

Submitted: 17 July 2006
Accepted: 30 November 2006

References

Brunet, S., and B. Maro. 2005. Cytoskeleton and cell cycle control during meiotic maturation of the mouse oocyte: integrating time and space. *Reproduction*. 130:801–811.

Chang, H.Y., M. Levasseur, and K.T. Jones. 2004. Degradation of APCcdc20 and APCcdh1 substrates during the second meiotic division in mouse eggs. *J. Cell Sci.* 117:6289–6296.

Choi, T., F. Aoki, M. Mori, M. Yamashita, Y. Nagahama, and K. Kohmoto. 1991. Activation of p34cdc2 protein kinase activity in meiotic and mitotic cell cycles in mouse oocytes and embryos. *Development*. 113:789–795.

Cleveland, D.W., Y. Mao, and K.F. Sullivan. 2003. Centromeres and kinetochores: from epigenetics to mitotic checkpoint signaling. *Cell*. 112:407–421.

Davis, M., A. Hatzubai, J.S. Andersen, E. Ben-Shushan, G.Z. Fisher, A. Yaron, A. Bauskin, F. Mercurio, M. Mann, and Y. Ben-Neriah. 2002. Pseudosubstrate regulation of the SCF(beta-TrCP) ubiquitin ligase by hnRNP-U. *Genes Dev.* 16:439–451.

Draetta, G., F. Luca, J. Westendorf, L. Brizuela, J. Ruderman, and D. Beach. 1989. Cdc2 protein kinase is complexed with both cyclin A and B: evidence for proteolytic inactivation of MPF. *Cell*. 56:829–838.

Fang, G. 2002. Checkpoint protein BubR1 acts synergistically with Mad2 to inhibit anaphase-promoting complex. *Mol. Biol. Cell*. 13:755–766.

Fang, G., H. Yu, and M.W. Kirschner. 1998. The checkpoint protein MAD2 and the mitotic regulator CDC20 form a ternary complex with the anaphase-promoting complex to control anaphase initiation. *Genes Dev.* 12:1871–1883.

Fang, G., H. Yu, and M.W. Kirschner. 1999. Control of mitotic transitions by the anaphase-promoting complex. *Philos. Trans. R. Soc. Lond. B Biol. Sci.* 354:1583–1590.

Felix, M.A., J.C. Labbe, M. Doree, T. Hunt, and E. Karsenti. 1990. Triggering of cyclin degradation in interphase extracts of amphibian eggs by cdc2 kinase. *Nature*. 346:379–382.

Gautier, J., J. Minshull, M. Lohka, M. Glotzer, T. Hunt, and J.L. Maller. 1990. Cyclin is a component of maturation-promoting factor from *Xenopus*. *Cell*. 60:487–494.

Glotzer, M., A.W. Murray, and M.W. Kirschner. 1991. Cyclin is degraded by the ubiquitin pathway. *Nature*. 349:132–138.

Golan, A., Y. Yudkovsky, and A. Hershko. 2002. The cyclin-ubiquitin ligase activity of cyclosome/APC is jointly activated by protein kinases Cdk1-cyclin B and Plk. *J. Biol. Chem.* 277:15552–15557.

Grosskortenhaus, R., and F. Sprenger. 2002. Rca1 inhibits APC-Cdh1(Fzr) and is required to prevent cyclin degradation in G2. *Dev. Cell*. 2:29–40.

Guardavaccaro, D., Y. Kudo, J. Boulaire, M. Barchi, L. Busino, M. Donzelli, F. Margottin-Goguet, P.K. Jackson, L. Yamasaki, and M. Pagano. 2003. Control of meiotic and mitotic progression by the F box protein beta-Trcp1 in vivo. *Dev. Cell*. 4:799–812.

Hansen, D.V., A.V. Loktev, K.H. Ban, and P.K. Jackson. 2004. Plk1 regulates activation of the anaphase promoting complex by phosphorylating and triggering SCFbetaTrCP-dependent destruction of the APC inhibitor Emi1. *Mol. Biol. Cell*. 15:5623–5634.

Hansen, D.V., J.J. Tung, and P.K. Jackson. 2006. CaMKII and polo-like kinase 1 sequentially phosphorylate the cytostatic factor Emi2/XErp1 to trigger its destruction and meiotic exit. *Proc. Natl. Acad. Sci. USA*. 103:608–613.

Hashimoto, N., and T. Kishimoto. 1986. Cell cycle dynamics of maturation-promoting factor during mouse oocyte maturation. *Tokai J. Exp. Clin. Med.* 11:471–477.

Herbert, M., M. Levasseur, H. Homer, K. Yallop, A. Murdoch, and A. McDougall. 2003. Homologue disjunction in mouse oocytes requires proteolysis of securin and cyclin B1. *Nat. Cell Biol.* 5:1023–1025.

Homer, H.A., A. McDougall, M. Levasseur, K. Yallop, A.P. Murdoch, and M. Herbert. 2005. Mad2 prevents aneuploidy and premature proteolysis of cyclin B and securin during meiosis I in mouse oocytes. *Genes Dev.* 19:202–207.

Hsu, J.Y., J.D. Reimann, C.S. Sorensen, J. Lukas, and P.K. Jackson. 2002. E2F-dependent accumulation of hEmi1 regulates S phase entry by inhibiting APC(Cdh1). *Nat. Cell Biol.* 4:358–366.

King, R.W., R.J. Deshaies, J.M. Peters, and M.W. Kirschner. 1996. How proteolysis drives the cell cycle. *Science*. 274:1652–1659.

Kramer, E.R., C. Gieffers, G. Holzl, M. Hengstschlager, and J.M. Peters. 1998. Activation of the human anaphase-promoting complex by proteins of the CDC20/Fizzy family. *Curr. Biol.* 8:1207–1210.

Kubiak, J.Z., M. Weber, H. de Pennart, N.J. Winston, and B. Maro. 1993. The metaphase II arrest in mouse oocytes is controlled through microtubule-dependent destruction of cyclin B in the presence of CSF. *EMBO J.* 12:3773–3778.

Labbe, J.C., J.P. Capony, D. Caput, J.C. Cavadore, J. Derancourt, M. Kaghad, J.M. Lelias, A. Picard, and M. Doree. 1989. MPF from starfish oocytes at first meiotic metaphase is a heterodimer containing one molecule of cdc2 and one molecule of cyclin B. *EMBO J.* 8:3053–3058.

Laemmli, U.K. 1970. Cleavage of structural proteins during the assembly of the head of bacteriophage T4. *Nature*. 227:680–685.

Lawitts, J.A., and J.D. Biggers. 1993. Culture of preimplantation embryos. *Methods Enzymol.* 225:153–164.

Ledan, E., Z. Polanski, M.E. Terret, and B. Maro. 2001. Meiotic maturation of the mouse oocyte requires an equilibrium between cyclin B synthesis and degradation. *Dev. Biol.* 232:400–413.

Li, X., and R.B. Nicklas. 1995. Mitotic forces control a cell-cycle checkpoint. *Nature*. 373:630–632.

Liu, J., and J.L. Maller. 2005. Calcium elevation at fertilization coordinates phosphorylation of XErp1/Emi2 by Plx1 and CaMK II to release metaphase arrest by cytostatic factor. *Curr. Biol.* 15:1458–1468.

Lorca, T., A. Castro, A.M. Martinez, S. Vigneron, N. Morin, S. Sigrist, C. Lehner, M. Doree, and J.C. Labbe. 1998. Fizzy is required for activation of the APC/cyclosome in *Xenopus* egg extracts. *EMBO J.* 17:3565–3575.

Madgwick, S., D.V. Hansen, M. Levasseur, P.K. Jackson, and K.T. Jones. 2006. Mouse Emi2 is required to enter meiosis II by reestablishing cyclin B1 during interkinesis. *J. Cell Biol.* 174:791–801.

Marangos, P., and J. Carroll. 2004a. Fertilization and InsP3-induced Ca2+ release stimulate a persistent increase in the rate of degradation of cyclin B1 specifically in mature mouse oocytes. *Dev. Biol.* 272:26–38.

Marangos, P., and J. Carroll. 2004b. The dynamics of cyclin B1 distribution during meiosis I in mouse oocytes. *Reproduction*. 128:153–162.

Marangos, P., G. Fitzharris, and J. Carroll. 2003. Ca2+ oscillations at fertilization in mammals are regulated by the formation of pronuclei. *Development*. 130:1461–1472.

Margottin-Goguet, F., J.Y. Hsu, A. Loktev, H.M. Hsieh, J.D. Reimann, and P.K. Jackson. 2003. Prophase destruction of Emi1 by the SCF(betaTrCP/Slimb) ubiquitin ligase activates the anaphase promoting complex to allow progression beyond prometaphase. *Dev. Cell*. 4:813–826.

Masui, Y., and C.L. Markert. 1971. Cytoplasmic control of nuclear behavior during meiotic maturation of frog oocytes. *J. Exp. Zool.* 177:129–145.

Moshe, Y., J. Boulaire, M. Pagano, and A. Hershko. 2004. Role of Polo-like kinase in the degradation of early mitotic inhibitor 1, a regulator of the

anaphase promoting complex/cyclosome. *Proc. Natl. Acad. Sci. USA*. 101:7937–7942.

Ohsumi, K., A. Koyanagi, T.M. Yamamoto, T. Gotoh, and T. Kishimoto. 2004. Emi1-mediated M-phase arrest in *Xenopus* eggs is distinct from cytostatic factor arrest. *Proc. Natl. Acad. Sci. USA*. 101:12531–12536.

Paronetto, M.P., E. Giorda, R. Carsetti, P. Rossi, R. Geremia, and C. Sette. 2004. Functional interaction between p90Rsk2 and Emi1 contributes to the metaphase arrest of mouse oocytes. *EMBO J.* 23:4649–4659.

Peter, M., A. Castro, T. Lorca, C. Le Peuch, L. Magnaghi-Jaulin, M. Doree, and J.C. Labbe. 2001. The APC is dispensable for first meiotic anaphase in *Xenopus* oocytes. *Nat. Cell Biol.* 3:83–87.

Peters, J.M. 2002. The anaphase-promoting complex: proteolysis in mitosis and beyond. *Mol. Cell*. 9:931–943.

Polanski, Z., E. Ledan, S. Brunet, S. Louvet, M.H. Verlhac, J.Z. Kubiak, and B. Maro. 1998. Cyclin synthesis controls the progression of meiotic maturation in mouse oocytes. *Development*. 125:4989–4997.

Raff, J.W., K. Jeffers, and J.Y. Huang. 2002. The roles of Fzy/Cdc20 and Fzr/Cdh1 in regulating the destruction of cyclin B in space and time. *J. Cell Biol.* 157:1139–1149.

Rauh, N.R., A. Schmidt, J. Bormann, E.A. Nigg, and T.U. Mayer. 2005. Calcium triggers exit from meiosis II by targeting the APC/C inhibitor XErp1 for degradation. *Nature*. 437:1048–1052.

Reimann, J.D., and P.K. Jackson. 2002. Emi1 is required for cytostatic factor arrest in vertebrate eggs. *Nature*. 416:850–854.

Reimann, J.D., E. Freed, J.Y. Hsu, E.R. Kramer, J.M. Peters, and P.K. Jackson. 2001a. Emi1 is a mitotic regulator that interacts with Cdc20 and inhibits the anaphase promoting complex. *Cell*. 105:645–655.

Reimann, J.D., B.E. Gardner, F. Margottin-Goguet, and P.K. Jackson. 2001b. Emi1 regulates the anaphase-promoting complex by a different mechanism than Mad2 proteins. *Genes Dev.* 15:3278–3285.

Reis, A., H.Y. Chang, M. Levasseur, and K.T. Jones. 2006. APCcdh1 activity in mouse oocytes prevents entry into the first meiotic division. *Nat. Cell Biol.* 8:539–540.

Shoji, S., N. Yoshida, M. Amanai, M. Ohgishi, T. Fukui, S. Fujimoto, Y. Nakano, E. Kajikawa, and A.C. Perry. 2006. Mammalian Emi2 mediates cytostatic arrest and transduces the signal for meiotic exit via Cdc20. *EMBO J.* 25:834–845.

Tay, J., R. Hodgman, and J.D. Richter. 2000. The control of cyclin B1 mRNA translation during mouse oocyte maturation. *Dev. Biol.* 221:1–9.

Terret, M.E., K. Wassmann, I. Waizenegger, B. Maro, J.M. Peters, and M.H. Verlhac. 2003. The meiosis I-to-meiosis II transition in mouse oocytes requires separase activity. *Curr. Biol.* 13:1797–1802.

Tung, J.J., and P.K. Jackson. 2005. Emi1 class of proteins regulate entry into meiosis and the meiosis I to meiosis II transition in *Xenopus* oocytes. *Cell Cycle*. 4:478–482.

Tung, J.J., D.V. Hansen, K.H. Ban, A.V. Loktev, M.K. Summers, J.R. Adler III, and P.K. Jackson. 2005. A role for the anaphase-promoting complex inhibitor Emi2/XErp1, a homolog of early mitotic inhibitor 1, in cytostatic factor arrest of *Xenopus* eggs. *Proc. Natl. Acad. Sci. USA*. 102:4318–4323.

Tunquist, B.J., and J.L. Maller. 2003. Under arrest: cytostatic factor (CSF)-mediated metaphase arrest in vertebrate eggs. *Genes Dev.* 17:683–710.

Wassmann, K., T. Niault, and B. Maro. 2003. Metaphase I arrest upon activation of the Mad2-dependent spindle checkpoint in mouse oocytes. *Curr. Biol.* 13:1596–1608.

Zachariae, W., and K. Nasmyth. 1999. Whose end is destruction: cell division and the anaphase-promoting complex. *Genes Dev.* 13:2039–2058.